Nanoscale Advances

ROYAL SOCIETY OF CHEMISTRY

COMMUNICATION

View Article Online
View Journal | View Issue

Cite this: *Nanoscale Adv.*, 2021, **3**, 6379

Received 22nd July 2021
Accepted 12th September 2021

DOI: 10.1039/d1na00568e

rsc.li/nanoscale-advances

Inhibition of cardiomyocyte apoptosis post-acute myocardial infarction through the efficient delivery of microRNA-24 by silica nanoparticles†

Hong Yu,[ae] Yi Li,[b] Ruirui Zhang,[c] Mengchen Shen,[d] Yuting Zhu,[e] Qiang Zhang,[e] Huiliang Liu,[ab] Dong Han,[ef] Xiaoli Shi*[ef] and Jiao Zhang*[a]

MicroRNA-24 (miR-24) is an apoptosis suppressor miRNA down-regulated in cardiomyocytes after acute myocardial infarction (AMI). However, due to the lack of effective delivery strategies, the role of anti-apoptotic miR-24 in cardiomyocytes post-acute myocardial infarction remains unexplored. Here, we used a silica nanoparticle-based polyelectrolyte (polyethylenimine, PEI) delivery system to study the role of miR-24. These particles with good biocompatibility could be efficiently internalized into cells and release the loaded miR-24 into the cytoplasm. As a result, the overexpression of miR-24 resulted in the inhibition of the pro-apoptotic Bim, thereby inhibiting cardiomyocyte apoptosis *in vitro*. Furthermore, *in vivo* experiments revealed that over-expressed miR-24 additionally significantly improves ventricular remodeling and cardiac function in Sprague–Dawley (SD) rats after coronary artery ligation. In summary, our novel delivery system serves as a therapeutic miRNA formulation for cardiovascular disease treatment.

In the early stages of acute myocardial infarction (AMI), cardiomyocytes tend to undergo apoptosis because of changes in the peripheral microenvironment[1,2] due to the oxidation-anti-oxidation imbalance of myocardial tissue caused by ischemia and hypoxia. Previous basic and clinical studies have shown that inhibition of cardiomyocyte apoptosis has a favorable effect on the heart, leading to new ideas to prevent or control acute myocardial infarction, improve ventricular remodeling, and protect cardiac function.[3–6] MicroRNAs (miRNAs) are endogenous small single-stranded non-coding RNAs that regulate gene expression at the post-transcriptional level. Numerous studies have shown that miR-24 effectively improves cardiac function and long-term prognosis,[7–10] post- acute myocardial infarction, by directly targeting the pro-apoptotic protein Bim, thereby significantly inhibiting cardiomyocyte apoptosis and fibrosis. Therefore, gene therapy with miRNA is expected to provide a new strategy for anti-apoptotic therapy. The goal of gene therapy is to successfully introduce genetic drugs (such as nucleic acids) into target cells to replace or repair target genes that cause specific diseases. Therefore, the successful transport of functional miRNA molecules into target cells is critical in initiating the regulation of gene expression processes.

RNA molecules are known to be highly unstable in cellular environments. A widely used approach to transport the chemically synthesized miRNA mimics/miRNA inhibitors into the cytoplasm of target cells is through delivery vectors categorized as viral and non-viral.[11] Despite a high transfection efficiency,[12] clinical applications of viral vectors such as lentiviruses and adenoviruses remain limited due to their tendency to trigger cell mutation, immune rejection, and potential carcinogenic risk. The transfection efficiency of liposomes,[13] a commonly used non-viral transport vector, is low for primary cells despite being relatively non-toxic. Nanomaterial-based gene therapy vectors have become increasingly successful over recent years. Silica nanoparticles, being easily surface-functionalized and suitable for carrying small molecule and macromolecule drugs such as RNA,[14–16] are particularly promising. Furthermore, recent studies have also shown that silica nanoparticles possess excellent biocompatibility when applied to mammalian cells.[17–19] However, the role of silica nanoparticles for the delivery of miRNAs for gene therapy of primitive cardiomyocytes remains largely unexplored.

In this study, we designed and prepared a silica nanoparticle system to deliver miR-24 for miRNA replacement therapy in

[a]*Department of Cardiology, Beijing Electric Power Hospital, State Grid Corporation of China, Beijing, 100078, P. R. China. E-mail: 15011558161@163.com*

[b]*Senior Department of Cardiology, The Sixth Medical Center of PLA General Hospital, Beijing, 100048, P. R. China*

[c]*College of Chemistry, Chemical Engineering and Materials Science, Key Laboratory of Molecular and Nano Probes, Ministry of Education, Shandong Provincial Key Laboratory of Clean Production of Fine Chemicals, Shandong Normal University, Jinan, 250014, P. R. China*

[d]*Graduate School of Anhui Medical University, Hefei, 230032, P. R. China*

[e]*CAS Center for Excellence in Nanoscience, National Center for Nanoscience and Technology, Beijing 100190, P. R. China. E-mail: shixl@nanoctr.cn*

[f]*School of Future Technology, University of Chinese Academy of Sciences, Beijing, 100049, P. R. China*

† Electronic supplementary information (ESI) available. See DOI: 10.1039/d1na00568e

cardiomyocytes in an acute myocardial infarction scenario. Here, we first proposed a method for covalently linking dithiobis(succinimidyl propionate) (DSP) to polyethylenimine (PEI). Then, we constructed functionalized silica nanoparticles (F-silica) by noncovalently modifying DSP–PEI on the surface of nanoparticles. Lastly, a gene carrier complex (F-silica-miR-24) was synthesized by electrostatic interaction with miR-24. We demonstrated that the nanoparticles exhibit high cellular uptake efficiency and successfully preserve miR-24's biological function. Furthermore, our study highlights a novel finding that F-silica-miR-24 is highly effective as miR-24 replacement therapy with good biocompatibility withthe host rat primary cardiomyocytes and rat MI models. Our results suggest that manipulating miRNA levels during stress-induced apoptosis may be an effective novel therapeutic strategy for treating cardiac diseases.

Silica nanoparticles were prepared using the reverse microemulsion method,[20] as described in the methods section. These nanoparticles are spherical and have a mean diameter of approximately 50 nm, as measured by TEM (Fig. 1A) and a mean hydrodynamic diameter of 40–60 nm as measured by DLS (Fig. 1B). The silica nanoparticles were then noncovalently functionalized with DSP–PEI (denoted as F-silica). Before this task, we already synthesized DSP–PEI by covalently connecting DSP and PEI. PEI has become a trusted RNA transfection agent over the years due to its dual properties to bind to nucleic acids and induce endosomal rupture *via* the traditional "proton-sponge" effect. However, unmodified PEI is ineffective in delivering RNA into the cells. Compared with pure PEI, F-silica has many biodegradable chemical bonds, such as disulfide bonds, which can be degraded into low toxicity or non-toxic ones *in vivo*. Colloidal stability of F-silica complexes is essential for effective miRNA delivery, and the zeta potential is an indicator of colloidal stability.[21] The zeta potential of F-silica is determined by calculating the ratio of silica nanoparticles to DSP–PEI. As shown in Fig. 1C, the increase of the mass ratio (W/W) also increased the zeta potential of F-silica gradually from -20.1 ± 0.52 to $+29.8 \pm 0.70$ mV. However, our experiments also indicated the presence of an excessively high positive charge, quickly causing aggregation among the complexes to form larger particle sizes and lower stability. Eventually, this led to the release of RNA from the complexes in advance and degradation by nucleases. Previous studies have shown that a positively charged complex easily adsorbs serum albumin and other harmful proteins to form large aggregates, cleared from the body by phagocytes.[22] Therefore, in our subsequent experiments we constructed F-silica according to the scheme with a mass ratio of 1 : 1 when the zeta potential remains at $+21.5 \pm 0.18$ mV, which is enough for carrying the miRNA.

It is known that electrostatic interactions are an effective way to complex anionic nucleic acids. Next, we evaluated the miR-24 protective capability of the vectors by agarose gel electrophoretic analysis before applying F-silica-miR-24 delivery vehicles to cells. We combined different final concentrations of F-silica (Fig. 1D) with the same final concentration of miRNA-24 (200 nM) by electrostatic adsorption. We observed a distinct fluorescent band for the pure miR-24 group (naked miRNA, lane 1). In contrast, a gradual increase in the F-silica concentration caused a subsequent decrease in the fluorescence intensity of the electrophoresis band. Furthermore, we noticed that at 0.25 mg mL^{-1} (lane 6), the band is entirely undetectable, suggesting that there is no free miR-24 in the supernatant at this concentration, and indirectly indicating that the nanoparticles are entirely loaded with 200 nM miR-24. Therefore, the loading efficiency of miR-24 bound to F-silica nanoparticles is 100%. Using this strategy, we synthesized and tested the efficacy of five formulations of F-silica-24 polyelectrolyte complexes to determine the best formulation for miRNA delivery.

It is reported that conventional methods such as lipofection and lentiviral/retroviral-mediated delivery with harmful polybrene are significantly toxic to the cells. Thus, our next aim was to evaluate the extent of the toxic effect of different concentrations of F-silica complexes on primary cardiomyocytes obtained from neonatal rat ventricular myocytes (NRVMs) by live-dead staining of cultures from days 1 and 3. Cardiomyocytes were extracted from 1 day-old Sprague–Dawley rats according to our previously described method.[23] As shown in Fig. 1E, the fluorescence of the living cells (green) and the dead cells (red), and the total green fluorescence on day 3 are substantially higher than the that of day one cells with a better elongation pattern. Also, no significant difference in the ratio of live cells between day 1 (Fig. 1F) and day 3 (Fig. 1G) was observed ($P > 0.05$) when the concentration of F-silica was lower than 0.6 mg mL^{-1}. Previous studies have confirmed that PEI transfection efficiency and toxicity are positively correlated with its molecular weight.[21] Therefore, in this study, we used DSP to transesterify the primary ammonia carried by PEI, thereby connecting PEI (800 Da) molecules to each other. Hence the resulting high molecular weight PEI displayed more biodegradable chemical bonds like ester bonds, carbon–nitrogen double bonds, or disulfide bonds *in vivo* than the regular sizeable molecular weight PEI. Moreover, these bonds show more characteristic degradation into less-toxic or non-toxic small molecular weight PEI than the simple large molecular weight PEI. Furthermore, the cell viability assays showed that F-silica had good biocompatibility and showed no significant effect on the viability of cardiomyocytes when co-cultured with cardiomyocytes for day 1/day 3 when the concentration of F-silica was lower than 0.6 mg mL^{-1}. Combined with the agarose gel electrophoresis results, we found that the nanoparticles are entirely loaded with 200 nM miR-24 at the concentration of 0.25 mg mL^{-1}. These observations collectively led us to use this concentration as the final concentration (0.25 mg mL^{-1}) of F-silica in the subsequent experiments.

To study whether F-silica can deliver miRNA into cardiomyocytes efficiently, we investigated the extent of the cellular uptake of FAM-labeled miR-24 (F-silica-miR-24) by fluorescence microscopy. As shown in Fig. 2A, the positions of miR-24 and nuclei in the cells are indicated by green and blue fluorescence, respectively. A comparative analysis of the nuclear and miR-24 localization by studying the distribution of green fluorescence indicated the successful delivery of miR-24 into the cell rather than being deposited on the cell's external surface. The naked miR-24 group could hardly detect green fluorescent spots,

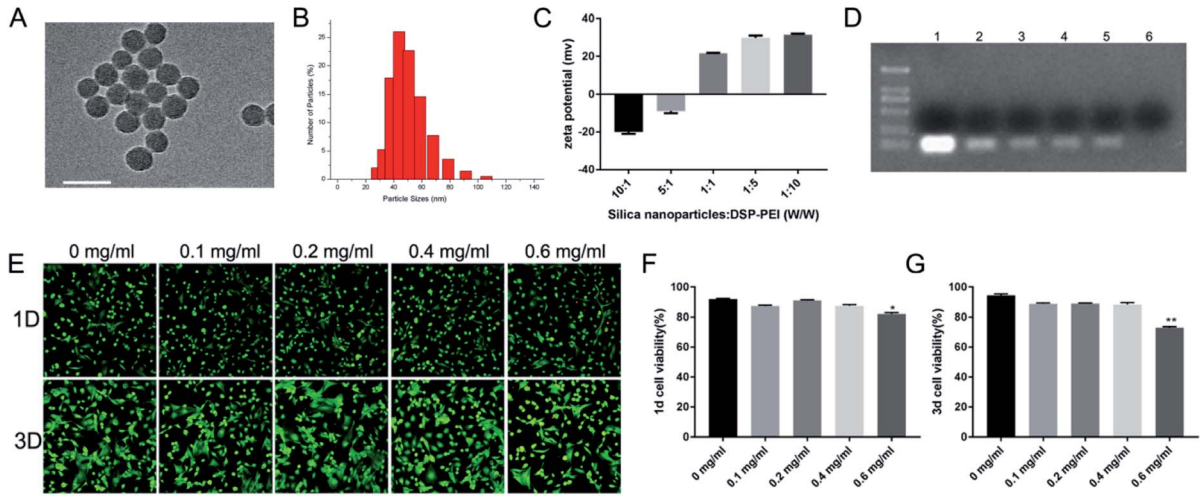

Fig. 1 Synthesis and characterization of silica nanoparticles: (A) transmission electron microscopy (TEM) images of silica nanoparticles (bars = 100 nm). (B) Dynamic light scattering (DLS) measurement results of silica nanoparticles. (C) Zeta potential of F-silica at different mass ratios. With an increase in the mass ratio (W/W), the zeta potential of F-silica gradually increases. (D) The binding stability of miRNA to F-silica was determined by agarose gel electrophoresis analysis. (E) The cell viability was detected by live/dead staining on day one and day 3. (F and G) Quantification of the dead cells compared with the control (without F-silica treatment). (*$p < 0.05$ and **$p < 0.01$).

indicating that RNase inside the cells efficiently degraded it. However, compared with the PEI-miR-24 group, the green fluorescent spots detected by the F-silica group were significantly more pronounced, indicating that the unmodified PEI-mediated miRNA transfection efficiency is very low. In the F-silica-miR-24 group, a transfection efficiency of 78% was determined according to the number of cells with green fluorescence. The cellular uptake study observations helped us to concretely conclude that the F-silica-miR-24 nanocarriers were highly efficient in delivering their cargo.

In the above experiment, we demonstrated that miRNAs could be efficiently delivered and released inside living cells. Next, we determined whether miRNAs delivered and released from F-silica-miR-24 complexes can retain their functionality *in vitro*. Therefore, we first examined the effect of H_2O_2 induced cytotoxicity in cardiomyocytes. For this, 100 μM H_2O_2 was added to cardiomyocyte culture for 0, 6, 12, 24, or 48 h, and the cell viability was assessed using a CCK-8 assay. The results showed that 6, 12, 24, or 48 h treatment of 100 μM H_2O_2 induced significant cell death among cardiomyocytes with increased cytotoxicity in a time-dependent manner, as shown in Fig. 2B.

Next, we cultured rat primary cardiomyocytes *in vitro*. We transfected them with either chemically synthesized double-stranded oligonucleotides that mimic the function of

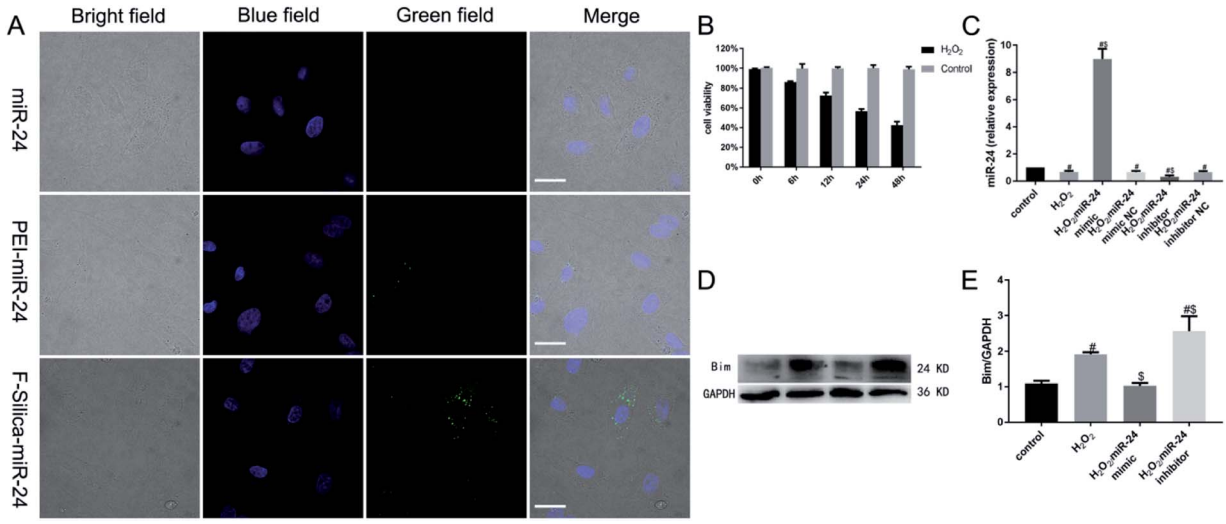

Fig. 2 Effect of miR-24 on apoptosis *in vitro*: (A) confocal images of cardiomyocytes transfected with naked miR-24, PEI-miR-24 and F-silica-miR-24. The nucleus was stained blue with DAPI, and miR-24 was labeled with green fluorescent FAM (bars = 20 μm). (B) A cell viability assay estimated the H_2O_2-induced cytotoxicity. (C) The expression of miR-24 was detected by real-time PCR. (D and E) The expression of Bim protein was detected by western blotting ($^{\#}p < 0.05$ compared with the control group; $^{\$}p < 0.05$ compared with the H_2O_2 group).

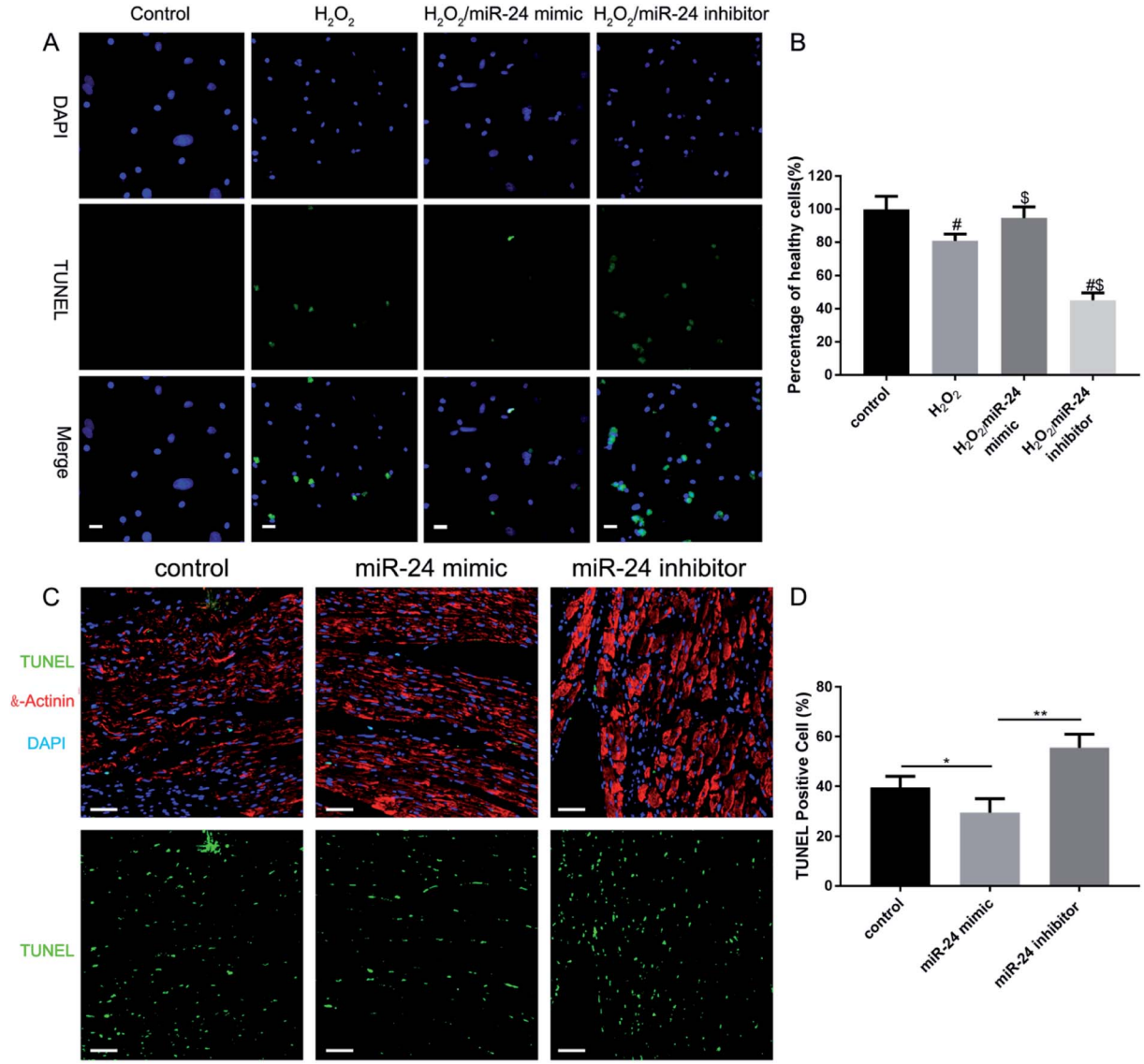

Fig. 3 Overexpression of miR-24 prevents cardiomyocyte apoptosis in response to H_2O_2. (A) Representative images of TUNEL staining of NRVMs show the apoptotic cells (nucleus stained in blue with DAPI and apoptotic cells stained in green) (bars = 20 μm). (B). Percentages of healthy (TUNEL-negative) cardiomyocytes were evaluated. ($^{\#}p < 0.05$ compared with the control group; $^{\$}p < 0.05$ compared with the H_2O_2 group). (C) After MI, the control or miR-24 mimic or miR-24 inhibitor was injected along the border zone of the infarcted area. Cardiomyocytes were co-immunostained for α-actinin to demonstrate the cardiomyocyte sarcomeres and gross morphology. DAPI was used for nuclear staining (bars = 50 μm). (D) Quantification of TUNEL-positive cardiomyocytes. Data were collected from rats in three independent experiments ($*p < 0.05$, $**p < 0.01$, and $n = 6$).

endogenous mature miR-24 (miR-24 mimic) or modified antisense oligoribonucleotides that inhibit miR-24 function (miR-24 inhibitor). Twenty-four hours after transfection, the cardiomyocytes were treated with 100 μM H_2O_2 for an additional 24 h to induce hypoxia-like cytotoxicity. Gene expression analysis showed that compared with the control group, the expression of miR-24 in myocardial cells of the H_2O_2-treated group, miR-24 mimic NC group, and miR-24 inhibitor NC group significantly decreased ($P < 0.05$) (Fig. 2C). This observation, consistent with the previous reports,[8] indicated that H_2O_2-induced cardiomyocyte apoptosis involved the downregulation of miR-24. However, the expression of miR-24 was significantly increased in the miR-24 mimic group and significantly decreased in the miR-24 inhibitor group ($P < 0.05$). These results collectively confirmed that the target specificity of the F-silica-delivered mature miRNAs was retained upon endosomal escape.

Subsequently, the western blotting analysis showed that compared with the control group, the pro-apoptotic target protein Bim expression in cardiomyocytes significantly increased in the H_2O_2-treated and the miR-24 inhibitor group ($P < 0.05$). However, Bim showed no significant expression difference in proteins between the control group and the miR-24

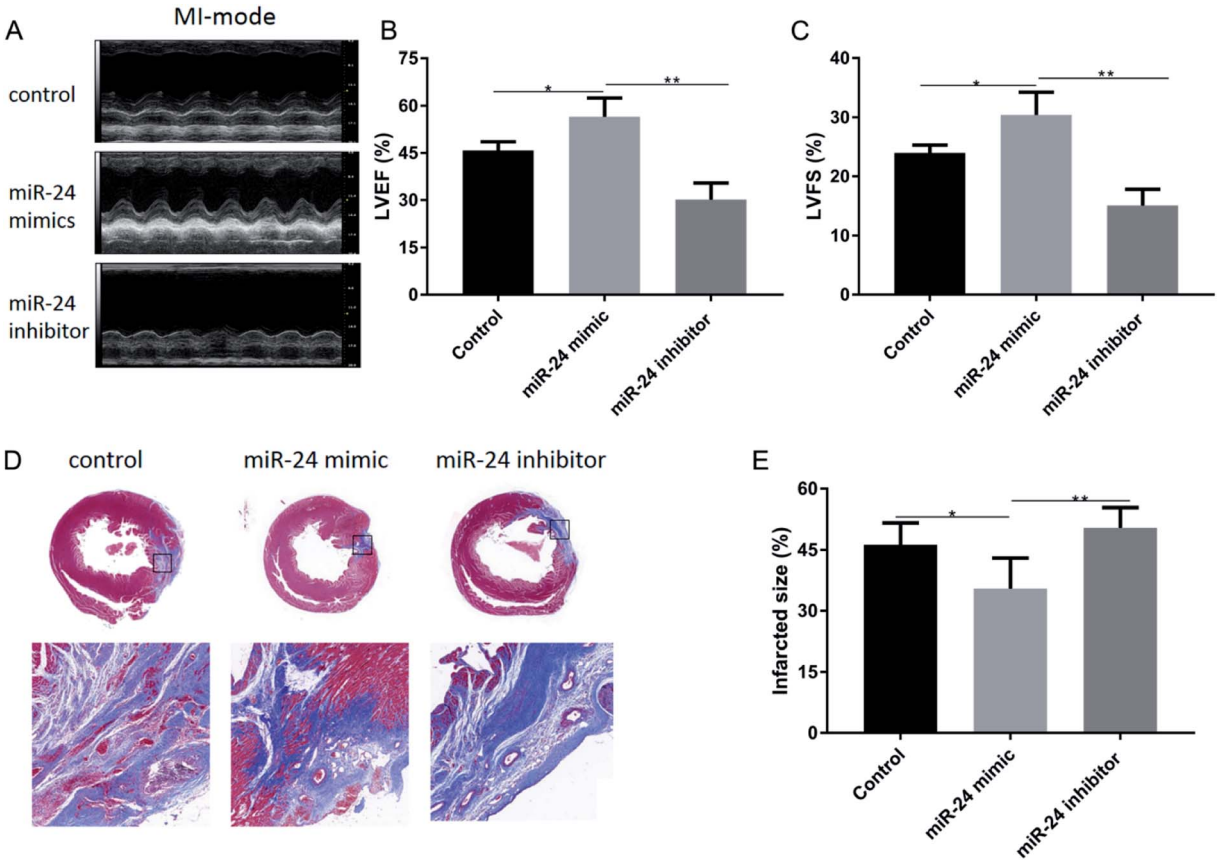

Fig. 4 (A) Cardiac function was evaluated by echocardiography two weeks after MI. (B and C) Both left ventricular shortening fraction (LVFS) and left ventricular ejection fraction (LVEF) were significantly improved in rats receiving the F-silica-miR-24 mimic injection compared with the other two groups. (D) Masson trichrome staining was performed on heart sections two weeks after MI with the control or miR-24 mimic or miR-24 inhibitor being injected. (E) Quantification of the infarct size. Data were collected from rats in three independent experiments (*$p < 0.05$, **$p < 0.01$, and $n = 6$).

mimic group ($P > 0.05$), further confirming the anti-apoptotic role of miR-24 (Fig. 2D–E).

To investigate the role of miR-24 in cardiomyocyte apoptosis regulation, we transfected the cells with 200 nM miR-24 mimic or miR-24 inhibitor to overexpress/down-regulate miR-24 in the cardiomyocytes. 24 h post-transfection, the cells were treated with 100 μM H_2O_2 for an additional 24 hours, followed by a TUNEL immunostaining assay to examine the effect of miR-24 on H_2O_2-induced cardiomyocyte apoptosis (Fig. 3A). More TUNEL-positive cells show H_2O_2 induced significant apoptosis in cardiomyocytes (Fig. 3B H_2O_2 *vs.* control). However, the overexpression of miR-24 significantly reduced the TUNEL-positive cardiomyocytes (Fig. 3B H_2O_2/miR-24-mimic *vs.* H_2O_2) while the knockdown of endogenous miR-24 significantly increased cardiomyocyte apoptosis (Fig. 3B H_2O_2/miR-24-inhibitor *vs.* H_2O_2). This observation conclusively indicated a direct anti-apoptotic role of miR-24 in cardiomyocytes post-AMI.

Next, we established our myocardial infarction model according to our previous research methods,[24] using male Sprague–Dawley (SD) rats (250 + 25 g) with permanent left anterior descending branch ligation. To further determine whether miR-24 mimic treatment could inhibit ischemia-induced apoptosis of cardiomyocytes *in vivo*, we adopted the following strategy. We combined TUNEL labeling (green fluorescence) with the cardiomyocyte marker α-actinin (red fluorescence) in infarcted mouse hearts 24 h after coronary artery ligation. At the same time, all the cell nuclei were labeled with DAPI (blue fluorescence) (Fig. 3C). Further, Fig. 3D shows that the TUNEL-positive cells (green fluorescent cells) were significantly higher in control and miR-24 inhibitor-treated groups than in the miR-24 mimic group ($p < 0.05$). All animal studies were approved by the Institutional Animal Care and Use Committee (IACUC) of the National Center for Nanoscience and Technology (Beijing, China).

Acute myocardial infarction in mice causes countless hemodynamic pressures, which trigger left ventricular remodeling, ultimately leading to functional decompensation and heart failure. Here, we hypothesized that a decrease in cardiac cell death by the action of the anti-apoptotic miR-24 would translate into improved cardiac function. Therefore, we assessed the cardiac function of the rats for two weeks post-coronary artery ligation by using echocardiography. All the rats showed a reduction in left ventricular function after

coronary artery ligation, confirming the successful induction of AMI (Fig. 4A). However, both LVEF (Fig. 4B) and LVFS (Fig. 4C) were significantly improved in the miR-24 mimic-treated group compared with the other groups ($p < 0.05$). Moreover, the infarct size, evaluated by Masson's trichrome staining of cardiac sections, showed a reduction in the scar size upon injection of miR-24, consistent with the improvement of cardiac function two weeks after AMI (Fig. 4D). As shown in (Fig. 4E), the infarct size of the control group, miR-24 mimic group, and miR-24 inhibitor group was 46.3 ± 2.693%, 35.5 ± 3.069%, and 50.42 ± 1.894%, respectively. The infarct size was significantly smaller in the miR-24 mimic group than in the other groups ($p < 0.05$).

Conclusions

In this study, our novel finding includes establishing a type of miRNA delivery system based on silica nanoparticles and cationic polyelectrolyte (PEI). The obtained F-silica-miR-24 vectors, can be readily internalized into the cells, with good biocompatibility and have incredibly efficient gene transfer efficiency (78%). Moreover, they efficiently escape from endo-lysosomes to successfully release the loaded miRNA molecules, thereby mediating a remarkable interference effect on the target gene (Bim) in cardiomyocytes cultured *in vitro*. By inhibiting the expression of Bim, we further demonstrated that our F-silica-miR-24 delivery system was efficient in inhibiting cardiomyocyte apoptosis *in vivo* in the early stage of acute myocardial infarction, thereby improving ventricular remodeling and long-term cardiac function. In summary, we have highlighted a novel theoretical basis for the potential future therapeutic use of nanomaterials to deliver miRNA *in vivo* to treat cardiovascular diseases.

Conflicts of interest

There are no conflicts to declare.

Acknowledgements

Hong Yu and Yi Li contributed equally to this work. This work was financially supported by the National Natural Science Foundation of China (Grant No. 31971317), Shandong Provincial Key Laboratory of Clean Production of Fine Chemicals (2019FCCEKL07), and the open foundation of Key Laboratory of Molecular and Nano Probes, Ministry of Education, Shandong Normal University (No. 2018KLMNP06).

Notes and references

1 B. Yu, F. Meng, Y. Yang, D. Liu and K. Shi, NOX2 Antisense Attenuates Hypoxia-Induced Oxidative Stress and Apoptosis in Cardiomyocyte, *Int. J. Med. Sci.*, 2016, **13**(8), 646–652.

2 L. Hou, J. Guo, F. Xu, X. Weng, W. Yue and J. Ge, Cardiomyocyte dimethylarginine dimethylaminohydrolase1 attenuates left-ventricular remodeling after acute myocardial infarction: involvement in oxidative stress and apoptosis, *Basic Res. Cardiol.*, 2018, **113**(4), 28.

3 C. Lin, Z. Liu, Y. Lu, *et al.* Cardioprotective effect of Salvianolic acid B on acute myocardial infarction by promoting autophagy and neovascularization and inhibiting apoptosis, *J. Pharm. Pharmacol.*, 2016, **68**(7), 941–952.

4 W. P. Cheng, H. M. Lo, B. W. Wang, S. K. Chua, M. J. Lu and K. G. Shyu, Atorvastatin alleviates cardiomyocyte apoptosis by suppressing TRB3 induced by acute myocardial infarction and hypoxia, *J. Formosan Med. Assoc.*, 2017, **116**(5), 388–397.

5 Z. Y. Shi, Y. Liu, L. Dong, *et al.* Cortistatin Improves Cardiac Function After Acute Myocardial Infarction in Rats by Suppressing Myocardial Apoptosis and Endoplasmic Reticulum Stress, *J. Cardiovasc. Pharmacol. Ther.*, 2017, **22**(1), 83–93.

6 F. Han, Q. Chen, J. Su, *et al.* MicroRNA-124 regulates cardiomyocyte apoptosis and myocardial infarction through targeting Dhcr24, *J. Mol. Cell. Cardiol.*, 2019, **132**, 178–188.

7 W. Minghua, G. Zhijian, H. Chahua, *et al.* Plasma exosomes induced by remote ischaemic preconditioning attenuate myocardial ischaemia/reperfusion injury by transferring miR-24, *Cell Death Discovery*, 2018, **9**(3), 320.

8 L. Qian, L. W. Van Laake, Y. Huang, S. Liu, M. F. Wendland and D. Srivastava, miR-24 inhibits apoptosis and represses Bim in mouse cardiomyocytes, *J. Exp. Med.*, 2011, **208**(3), 549–560.

9 D. Wang, X. Hu, S. H. Lee, *et al.* Diabetes Exacerbates Myocardial Ischemia/Reperfusion Injury by Down-Regulation of MicroRNA and Up-Regulation of *O*-GlcNAcylation, *JACC Basic Transl Sci*, 2018, **3**(3), 350–362.

10 L. Wang and L. Qian, miR-24 regulates intrinsic apoptosis pathway in mouse cardiomyocytes, *PLoS One*, 2014, **9**(1), e85389.

11 Y. Zhang, Z. Wang and R. A. Gemeinhart, Progress in microRNA delivery, *J. Controlled Release*, 2013, **172**(3), 962–974.

12 K. Lundstrom, RNA Viruses as Tools in Gene Therapy and Vaccine Development, *Genes*, 2019, **10**(3), 189.

13 L. Sercombe, T. Veerati, F. Moheimani, S. Y. Wu, A. K. Sood and S. Hua, Advances and Challenges of Liposome Assisted Drug Delivery, *Front. Pharmacol.*, 2015, **6**, 286.

14 N. A. Keasberry, C. W. Yapp and A. Idris, Mesoporous Silica Nanoparticles as a Carrier Platform for Intracellular Delivery of Nucleic Acids, *Biochemistry*, 2017, **82**(6), 655–662.

15 L. Xiong, J. Bi, Y. Tang and S. Z. Qiao, Magnetic Core–Shell Silica Nanoparticles with Large Radial Mesopores for siRNA Delivery, *Small*, 2016, **12**(34), 4735–4742.

16 J. Shen, H. Liu, C. Mu, *et al.* Multi-step encapsulation of chemotherapy and gene silencing agents in functionalized mesoporous silica nanoparticles, *Nanoscale*, 2017, **9**(16), 5329–5341.

17 C. M. Roberts, S. A. Shahin, W. Wen, *et al.* Nanoparticle delivery of siRNA against TWIST to reduce drug resistance

and tumor growth in ovarian cancer models, *Nanomedicine*, 2017, **13**(3), 965–976.

18 Y. Wang, Y. Xie, K. V. Kilchrist, J. Li, C. L. Duvall and D. Oupicky, Endosomolytic and Tumor-Penetrating Mesoporous Silica Nanoparticles for siRNA/miRNA Combination Cancer Therapy, *ACS Appl. Mater. Interfaces*, 2020, **12**(4), 4308–4322.

19 A. Bertucci, E. A. Prasetyanto, D. Septiadi, *et al.* Combined Delivery of Temozolomide and Anti-miR221 PNA Using Mesoporous Silica Nanoparticles Induces Apoptosis in Resistant Glioma Cells, *Small*, 2015, **11**(42), 5687–5695.

20 H. Li, Y. Mu, J. Lu, W. Wei, Y. Wan and S. Liu, Target-cell-specific fluorescence silica nanoprobes for imaging and theranostics of cancer cells, *Anal. Chem.*, 2014, **86**(7), 3602–3609.

21 M. A. Gosselin, W. Guo and R. J. Lee, Efficient gene transfer using reversibly cross-linked low molecular weight polyethylenimine, *Bioconjugate Chem.*, 2001, **12**(6), 989–994.

22 P. R. Dash, M. L. Read, L. B. Barrett, M. A. Wolfert and L. W. Seymour, Factors affecting blood clearance and *in vivo* distribution of polyelectrolyte complexes for gene delivery, *Gene Ther.*, 1999, **6**(4), 643–650.

23 Y. Li, X. Shi, L. Tian, *et al.* AuNP-Collagen Matrix with Localized Stiffness for Cardiac-Tissue Engineering: Enhancing the Assembly of Intercalated Discs by beta1-Integrin-Mediated Signaling, *Adv. Mater.*, 2016, **28**(46), 10230–10235.

24 R. Bai, L. Tian, Y. Li, *et al.* Combining ECM Hydrogels of Cardiac Bioactivity with Stem Cells of High Cardiomyogenic Potential for Myocardial Repair, *Stem Cells Int.*, 2019, **2019**, 6708435.